

Total Cross Sections for Negative and Positive Pions in Hydrogen and Deuterium*

J. ASHKIN, J. P. BLASER, F. FEINER, J. G. GORMAN,† AND M. O. STERN
Carnegie Institute of Technology, Pittsburgh, Pennsylvania

(Received July 2, 1954)

External meson beams, ranging in energy from 135 Mev to 260 Mev for the π^- , and 135 Mev to 198 Mev for the π^+ , have been used for the measurement of total cross sections by an attenuation experiment using liquid hydrogen as well as CH_2 and C as absorbers. Possible errors introduced by contamination of the π^+ beam by protons have been eliminated by use of time-of-flight and pulse-height discrimination. The corrected cross sections for π^- mesons in hydrogen rise from 47 mb at 133 Mev to a maximum of about 66 mb near 180 Mev and fall thereafter to 38 mb at 258 Mev, with typical uncertainties of ± 5 percent. The cross sections for π^+ mesons rise from 122 mb at 128 Mev to around 200 mb between 170 Mev and 196 Mev, with accuracy comparable to that for the π^- mesons except for the very high energies where the beams are of low intensity. The π^+ cross sections follow very well the curve representing three times the total π^- cross section, indicating that in the measured energy range the dominant interaction between pion and nucleon occurs for total isobaric spin $I = \frac{3}{2}$. Comparison of the π^- cross section with $(8/3)\pi\lambda^2$ supports the idea that the particular angular momentum state $J = \frac{3}{2}, L = 1$ (for $I = \frac{3}{2}$) is especially prominent in the scattering.

The total cross sections for π^+ and π^- mesons interacting with deuterium have also been measured by comparing the transmissions of D_2O and H_2O cells. Within the accuracy, the π^+ and π^- total cross sections are equal, consistent with the principle of charge symmetry. The total scattering cross section of deuterium is less than but of the same order of magnitude as the sum of the hydrogen cross sections for π^+ and π^- .

ATENUATION measurements, made at this laboratory, of the total interaction cross section of negative pions in hydrogen have been reported previously.¹ They give results in good agreement with the extensive work at Chicago,²⁻⁴ reaching up to 217 Mev for the pion energy, and extend the measurements to 260 Mev, well beyond the maximum in the total cross section.

Since then we have found it possible to obtain energetic positive pion beams from the synchrocyclotron which are weak in intensity but strong enough to allow a comparison of the positive pion cross section with that for negative pions up to an energy of 200 Mev. Such a comparison is essential in any attempt to discover the states of isobaric spin and angular momentum which are prominent in the scattering. The range of the present measurements is from 128 to 196 Mev for positive pions and 133 to 258 Mev for negative pions. We have also measured the total cross sections of deuterium by finding the difference in transmission of heavy water and ordinary water.

Following is a more detailed presentation of the results obtained and the methods used. The major part of the discussion is concerned with the hydrogen experiments. At the end there is a brief report of the

heavy water—ordinary water differences and their possible significance.

I. EXPERIMENTAL METHOD

A. General Arrangement

Figure 1 shows a plan view of the Carnegie Tech Cyclotron taken in the plane of the beam. The pions produced when the 440-Mev protons strike an internal copper or beryllium target are analyzed and focused by the fringing field of the cyclotron and enter the experimental area through channels in the lead and concrete shield wall, 8 feet thick. A 45° -sector deflecting magnet of aperture 4 in. \times 4 in. serves to purify the beam and provides double focusing of an incident parallel beam at a distance of two meters from the magnet exit. At a given channel set for the detection of negative pions, one can obtain a positive pion beam of the same energy, traversing the same trajectory but unfortunately greatly reduced in intensity, by reversing the direction of the circulating proton beam, thereby taking the pions produced in a backward direction with respect to the proton beam.

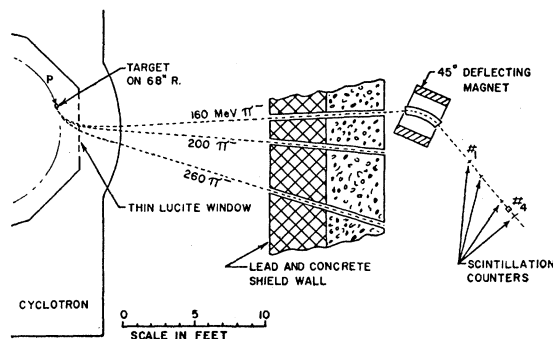


FIG. 1. General experimental arrangement.

* Research partially supported by the U. S. Atomic Energy Commission.

† A thesis based on this work has been submitted by J. G. Gorman in partial fulfillment of the requirements for the degree of Doctor of Philosophy at Carnegie Institute of Technology.

¹ Ashkin, Blaser, Feiner, Gorman, and Stern, Phys. Rev. **93**, 1129 (1954).

² Anderson, Fermi, Long, Martin, and Nagle, Phys. Rev. **85**, 934 (1952).

³ Fermi, Glicksman, Martin, and Nagle, Phys. Rev. **92**, 161 (1953).

⁴ M. Glicksman, Phys. Rev. **94**, 1335 (1954); the scattering of 187-Mev π^- mesons has also been measured (private communication).

For a measurement of total cross section, the pions are made to pass through a monitoring telescope of three scintillation counters in coincidence recording the number of particles incident, and then through an absorber (liquid hydrogen) to a fourth detecting counter, in coincidence with the monitor. The typical transmission geometry for the negative pion measurements is shown in Fig. 2. Ideally, the cross section is obtained by comparing the transmissions (ratio of quadruple coincidences, hereafter called Q , to triple coincidences, hereafter called T) with and without the absorber. Thus, if σ is the total cross section per atom of the absorber and N is the surface density of the absorber in atoms/cm²,

$$\exp(-N\sigma) = \frac{(Q/T)_{\text{absorber}}}{(Q/T)_{\text{no absorber}}} \quad (1)$$

In practice, the final cross section is obtained only after suitable corrections have been made for contamination of the pion beam, chance coincidences, scattering through small angles, etc., as we shall see in the following.

As far as possible, we have aimed at an over-all accuracy of three to five percent in the measurements.

B. Production and Composition of the Pion Beams

For producing the negative pions we used a beryllium target of dimensions 2 inches in the direction of the proton beam, $\frac{1}{2}$ inch high, and $\frac{1}{4}$ inch thick. The three-fold coincidence rate in the standard geometry, Fig. 2, ranged, in counts/min, from 100 000 for the 135-Mev negative pions to 2000 for the 260-Mev negative pions. For producing the positive pions a $\frac{3}{4}$ -inch by $\frac{1}{2}$ -inch by $\frac{1}{4}$ -inch copper element was used. The three-fold coincidence rate in the time-of-flight geometry, Fig. 6, ranged, in counts/min, from 5300 for the 135-Mev positive pions to 150 for the 198-Mev positive pions.

The choice of target was not based on a detailed study. But in comparing the above two, we found that the beryllium gave about five times the intensity of 260-Mev negative pions while the intensity at 135 Mev

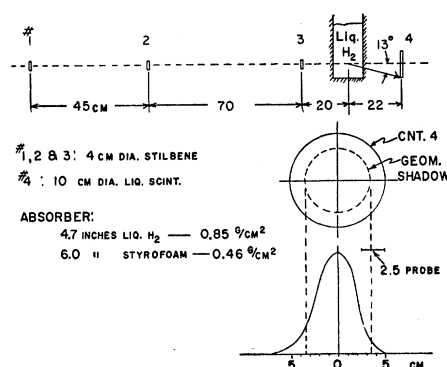


FIG. 2. Transmission geometry for the negative pion measurements. The curve represents the beam profile taken along the horizontal diameter of counter No. 4 (160-Mev π^- beam).

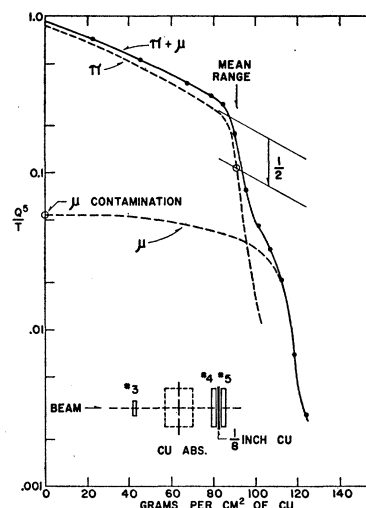


Fig. 3. Range curve of 194-Mev π^- mesons in copper, showing decomposition into pions and muons and construction of the mean range.

was the same. The copper gave about four times the intensity of positive pions at 160 Mev and usable intensities at higher energies where positive pions from the beryllium target escaped detection.

It is of course important to have a more precise indication of the energy of the pion beams than is provided by the nominal values associated with each channel. In addition the extent of the beam contamination has to be measured. For the negative pion beams, the principal contamination consists of muons of the same momentum following the pion trajectory, and a small fraction of electrons. For the positive pion beams, the major contamination consists of a very large number of low energy protons having the same momentum as the pions.

In order to determine the energy of the beams and the extent of the contaminations, we took integral range curves with copper absorber. For this purpose we used, besides the monitor, two detecting counters separated by a $\frac{1}{8}$ -inch copper absorber in the configuration indicated in the inset of Fig. 3. The effect of the additional counter and thin absorber was to discriminate against neutron and proton star fragments that might otherwise give a false indication especially near the end of the pion range. (Clean range curves were nevertheless taken with only one detecting counter in the case of the positive pion beams.)

Figure 3 represents a typical range curve and shows how the beam energy⁵ and the μ contamination are obtained graphically. The copper absorber was built up symmetrically about a fixed point (center of the total absorber required). This gives range curves with more constant initial slope. The two sharp drops in

⁵ We used the range-energy relation of W. A. Aron, University of California Radiation Laboratory Report UCRL-1325, 1951 (unpublished).

the curve are interpreted as the end of the range of pions and muons respectively.⁶ In order to determine the mean range of the pions and the fraction of muons present, the range curve has been split into π and μ components assuming that only multiple Coulomb scattering affects the μ mesons traversing the copper, whereas π mesons suffer in addition nuclear absorption and diffraction scattering. The slope at mean range has been taken as an indication of the spread in energy of the beam. Actually, the mean ranges determined in this way are a little too small since the path of the pion in the absorber is deviated from a straight line by multiple Coulomb scattering. A rough estimate indicates that the mean energies should be increased by about 1 percent on this account and this has been done for the energies listed in the tables showing the final results.

Electrons in a negative pion beam of 135 Mev were detected for the case that the copper target was used. The range curve, when compared with one for a beam of the same energy produced with the usual beryllium target, showed a pronounced penetrating tail, not previously encountered, and interpretable as a residue of electrons. The contaminated beam was estimated to have between 5 and 10 percent of electrons by comparing cross sections measured in the two beams. The absence of such tails in all range curves for the actual beams used justifies neglect of the electron contamination. This is consistent with the experience of Martin⁷ with the 450-Mev Chicago cyclotron.

As already mentioned, we discovered early in our investigation of the positive pion beams that especially those of high energy were very badly flooded with low-energy protons coming from the meson target and elsewhere in the cyclotron. Elimination of these protons was the major problem in the positive pion measurements and will be discussed in detail later in Sec. IV. The beams remaining after removal of the protons were analyzed by measuring integral range curves in the

manner previously described to give the energies and muon contaminations listed in Table VII. We found no evidence for any appreciable positron contamination of the beams in spite of the fact that the copper meson target was used. This is in agreement with measurements of Bodansky *et al.* at Columbia⁸ and shows that at the same energy the positive pion beams have much smaller electron contaminations than do the negative pion beams.⁹

C. Detection Equipment

For various practical reasons (see Sec. I D), the absorbers used in the measurements have been chosen of such a size that they produce relatively small changes in transmission, in some cases as small as two percent. To achieve an accuracy of something like three percent in the cross section, therefore, requires that the transmissions be reliably measured to better than one part in 1000. This puts rather stringent requirements on the detection apparatus. Small drifts in the electronic equipment, deadtime in the detection, background counts, etc., must be seriously considered for their effect on the final accuracy.

1. Stability

As shown in the block diagram of Fig. 4, the pulses from the scintillation counters are amplified in wide-band distributed amplifiers, then limited to about 1.5 volts and clipped by shorted stubs to a length of 8 μ sec. They are fed into a multiple coincidence circuit using crystal diodes,¹⁰ providing fast outputs for the monitor triples $T(123)$ and transmitted quadruples $Q(1234)$. In general these output pulses vary around a certain average height, the fluctuations being mainly due to time-jitter and statistical variations in ionization and photoelectron emission. In addition some mesons may traverse the edge of a counter and thereby produce smaller output pulses. Because of this inherent ambiguity in pulse size, the transmission Q/T , as obtained from direct counting of Q and T , depends on the settings of the T and Q output discriminators and will vary by as much as a percent if these discriminators undergo independent drift.

To avoid difficulties of this kind, the T and Q pulses, after their respective discriminators, are transformed by univibrators (using E F P-60 tubes¹¹) into pulses of constant shape and amplitude and subsequently put

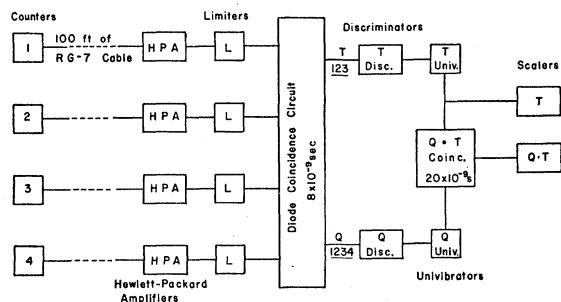


FIG. 4. Block diagram of the electronics.

⁶ Only μ mesons having traversed the focusing magnet have a defined range and can be detected by this method. μ mesons originating from π decays occurring after the focusing magnet could be hidden under the curve as they do not have a unique energy. As their number cannot exceed about 2 percent, their possible effect has been incorporated in the error attributed to the determination of the μ contamination.

⁷ R. L. Martin, Phys. Rev. **87**, 1052 (1952).

⁸ Bodansky, Sachs, and Steinberger, Phys. Rev. **93**, 1367 (1954).

⁹ The reason for this may be partly the large excess of positive over negative pions in the production process. π^+ to π^- ratios of 7 to 10 have been reported by M. M. Block *et al.*, Phys. Rev. **88**, 1239 (1952), and by A. H. Rosenfeld, Phys. Rev. **95**, 638 (A) (1954). Since the absolute number of electrons or positrons coming from the meson target should be proportional to the production of neutral pions, the relative number in the π^+ beam should be a factor 7 to 10 smaller than for the π^- .

¹⁰ S. DeBenedetti and H. J. Richings, Rev. Sci. Instr. **23**, 37 (1952).

¹¹ J. Fischer, University of Chicago (private communication).

into coincidence. The Q discriminator is adjusted so as to accept even very small Q pulses, whereas the T discriminator is set to reject the smaller pulses. By counting in this manner only those Q 's which have undergone the secondary Q - T coincidence, and by having T pulses of absolutely constant height, it is guaranteed that only those T 's are registered which also act as a possible coincidence partner for a Q and *vice versa*. The resulting ratio Q/T is found in practice to be quite insensitive to drift in either discriminator. Plateaus were obtained with a slope of 0.1 percent over a range of a factor 2 in the T pulse height whereas the T 's and Q 's alone had a slope of some 10 percent over the same range.

2. Deadtime Effects

The minimum interval in time for two pulses to be counted separately was of the order 0.2–0.3 μ sec, this being the deadtime of the univibrators. With the more intense negative pion beams, at intensities desirable for good statistics, the probability for one pion to be followed by another in this time span is several percent. The resulting counting losses would be inadmissibly large were it not for the effect of the secondary Q - T coincidence circuit.

If one makes the deadtime of the T univibrator the longer one, it is easy to see that the second of two mesons separated by an interval less than this deadtime is eliminated from further consideration by the failure of the T univibrator to send a pulse to the Q - T circuit. The ratio Q/T obtained this way is still correct up to the point where the spacing gets smaller than the resolving time of the secondary coincidence circuit. In the experiment, this time was 0.02 μ sec, thereby reducing the error to the cases where two mesons arrive within the same rf cycle (one revolution of the protons circulating with 20 Mc/sec inside the cyclotron). The resulting error was in all cases well below one percent. There is no effect of the 0.1- μ sec deadtime of the Hewlett-Packard scalars since all pulses reaching the scalars are spaced 0.3 μ sec or more apart.

3. Background

Background events in the monitor telescope will give T 's not originating from a complete meson traversal. As long as this rate does not vary, it will not affect the cross-section measurement. But if a few percent of the T 's are background events, any variation in machine operation producing a change of 0.1 percent in the contribution of the accidentals is harmful. By the use of three monitor counters it was possible to keep the accidental T 's well below one percent, thus avoiding any correction when the cyclotron was normally stable.

Background events in the Q 's result mainly from a meson traversing the monitor only and combining with a random count in counter No. 4. Since this happens only when the meson is not transmitted, the effect is

proportional to the attenuation. The corresponding correction to the cross section, listed under Accidentals in Table IV and Table VII, never exceeded three percent and was considered accurate to ± 1 percent.

The background rates were determined by inserting delay cables between different counters and the coincidence circuit.¹²

4. Scintillation Counters

The three small monitor counters used for the defining telescope each consist of a stilbene crystal 4 cm in diameter and 0.5 cm thick, viewed from the side by a single RCA 1P21 photomultiplier. The large monitor counter used in the time of flight method, Fig. 6, to be discussed later for the positive pion measurements, consists of a plastic scintillating disk¹³ 15 cm in diameter and 1 cm thick mounted with silicone grease in a Lucite holder following the design of Garwin.¹⁴ The pulse height variation over the face of the counter is less than 10 percent.

In all the negative pion measurements, the transmitted particles were detected with a liquid¹⁵ scintillation counter 10 cm in diameter and 2.5 cm thick, enclosed in a Lucite cell, Lucite serving as the light pipe to an RCA 5819. The response of the counter was uniform to within 10 percent. For the π -range curves, two such counters were used. In the positive pion measurements, which required pulse height selection and a better transmission geometry (see Fig. 6), we resorted to a single larger counter. This counter consisted of a plastic scintillating disk 20 cm in diameter, in optical contact at one face with a short Lucite light pipe leading to a DuMont 6292 photomultiplier. The scintillant was thus viewed end-on, the axis of the whole assembly coinciding with the beam. We used a DuMont tube because of its good pulse-height characteristics. In addition, the other face of the disk was machined to a spherically concave surface of such curvature as to give uniform pulses over the entire area of the counter.

D. Absorbers

In deciding on the thickness of absorber to use, it is necessary to make a balance between conflicting requirements. With a thick absorber the attenuation is large and therefore easier to measure accurately. On

¹² It should be noted however that it is not in general possible to find a configuration of delays which enables one to measure the background actually significant for the measurement. This is due to the presence in each counter of random counts, "bunched" counts (those having the periodicity of the circulating proton beam), as well as counts due to simultaneous traversals of several counters.

¹³ The plastic scintillator was made by the compression molding technique: G. G. Eichholz and J. L. Horwood, *Rev. Sci. Instr.* **23**, 305 (1952). We are especially indebted to F. Chen of the Brookhaven National Laboratory for detailed notes on this technique (unpublished).

¹⁴ R. L. Garwin, *Rev. Sci. Instr.* **23**, 755 (1952).

¹⁵ H. Kallman and M. Furst, *Phys. Rev.* **81**, 853 (1951).

TABLE I. Absorber data.

Absorber	Density, d g/cm ³	Atomic wt.	Thickness, l (cm)	Surface density g/cm ²	N (10 ²³ molecules/cm ²)
C	1.670	12.010	3.173	5.299	2.656
C'	1.670	12.010	4.357	7.276	3.647
CH ₂	0.913±0.2%	14.026	6.779±0.2%	6.189±0.35%	2.656±0.009
Liquid hyd.	0.0709	1.008	12.0±0.2	0.85 ±0.02	5.10 ±0.1 (atoms/cm ²)
Styrofoam	0.03	...	15.2	0.46	...
D ₂ O	1.111	20.03	6.447	7.163	2.155
H ₂ O	0.997	18.02	6.454	6.435	2.151

the other hand, the cross sections in hydrogen show a rather strong energy dependence so that it is advisable to minimize the energy loss of the primary pions in the target. In addition, the forward scattering corrections, discussed in Sec. III, would be even more uncertain for a target that is too long. As a reasonable compromise, we have chosen roughly five inches as the thickness of liquid hydrogen in the beam direction, giving a total energy loss of about 4 Mev for the pions in the hydrogen.

The liquid hydrogen is contained in the inner box (2.5-liter capacity) of a double-walled Styrofoam chamber¹⁶ with the hydrogen exhaust at the bottom of the outer box. With a useful volume of one liter in the region of the beam and an evaporation rate of about 1.3 liters per hour, the desired statistical accuracy in the transmission could usually be obtained with one or two fillings at a given energy. The inner box is lined with a one-mil copper form to prevent the hydrogen from touching the plastic and to define the path length better, although actually the walls shrink by a few percent when cooled to liquid hydrogen temperature. This shrinkage as well as bubbling in the liquid was checked by observing the inside of a similar chamber with clear Lucite covers during a filling and also by measuring the weight of the chamber against depth as the liquid evaporated. To within an uncertainty of ±2 percent, the surface density was measured as 0.85 g/cm² of hydrogen. This uncertainty is taken into account in the final error quoted on the cross sections but should not affect the relative values at different

energies. Table I contains the data for the hydrogen chamber.

For some of the transmission measurements we used a set of carbon and polyethylene (CH₂) absorbers. The absorber labeled C in Table I has the same surface density of carbon atoms as does the CH₂, while the one labeled C' has approximately the same stopping power as the CH₂.

The deuterium measurements, described in Sec. VI, were made with two nearly identical glass cells containing heavy water and water, respectively, as indicated in Table I.

II. CHOICE OF GEOMETRY

Because of unavoidable effects due to Coulomb scattering at small angles, it is never possible, with charged particles, to make transmission measurements in very good geometry. Although the multiple small-angle Coulomb scattering in hydrogen can generally be neglected,¹⁷ there remains the effect of single Coulomb scattering insofar as the Coulomb scattering amplitude interferes with the nuclear amplitude for the scattering of the pion. It is therefore essential to make the acceptance angle of the fourth transmission counter large enough so that pions scattered out are practically not affected by the Coulomb interference. To obtain the total nuclear cross section one must then supplement the experimental attenuation with some estimate, based on an assumed angular distribution, of the nuclear cross section for scattering into the acceptance cone of the last counter. It should be noted that with protons as the target nuclei, free to recoil, it is also necessary to estimate the cross section for protons to be projected forward so as to hit the last counter.

With these considerations in mind, the geometry used in the experiments was as follows. For all experiments with the negative pions, the relevant dimensions are indicated in Fig. 2 and Table II. We shall call this the π^- geometry. The half-angle θ subtended by the last counter (radius $R=5$ cm) at the center of the liquid hydrogen is 13° and the "shadow" cone, defined by rays traversing the extreme edges of the monitor counters, intersects the last counter in a circle of radius $r=3.5$ cm. The angular displacement δ from the edge of the shadow circle to the edge of the counter

TABLE II. Different transmission geometries. R is the radius of the last counter. θ is the half-angle subtended by the last counter at the center of the liquid hydrogen. r is the radius of the circular intersection of the last counter with the "shadow" cone, defined by rays traversing the extreme edges of the monitor counters. δ is the angular displacement from the edge of the shadow circle to the edge of the last counter, measured at the center of the hydrogen. P.H. = pulse-height method; T.F. = time-of-flight method.

Geometry	R cm	θ deg	r cm	δ deg
π^-	5	13°	3.5	4.0°
P.H. or T.F.	10	13°	4.3	7.5°
T.F.	10	6.4°	4.8	3.4°

¹⁶ We wish to thank L. Marshall for information about the Styrofoam target for liquid hydrogen which was used in connection with the proton-proton scattering experiments at Chicago.

¹⁷ The Gaussian distribution for the multiple scattering is characterized by a root-mean-square angle of 0.4 degrees or less.

corresponds to 4° measured at the center of the hydrogen. A pion passing along the axis of the counter system must therefore be scattered through more than 13° to contribute an attenuation, while a pion skimming the extreme edges of the monitor counters need be scattered only slightly more than 4° , but in a limited azimuthal range, to miss the detecting counter.

Because of the Coulomb force, the scattering cross section at 4° becomes quite large, about 60 mb/sterad in the present energy range, compared to 5 or 10 mb/sterad for the purely nuclear elastic scattering of π^- . However, only a small fraction of this scattering near 4° gives an attenuation since most of the 2π azimuth remains within the detecting counter. In addition only a very small fraction of the incident pions traverse the monitor counters near the edge of the shadow cone. This was observed directly by exploring one of the beams (160 Mev) with a 2.5 cm diameter probe counter in the plane of the last detecting counter. The intensity is concentrated in a region of about 2.5 cm vertical extent, with a horizontal variation as shown in Fig. 2. The beam is evidently well concentrated near the central axis. In the neighborhood of 13° it is possible to show from the known angular distributions and estimated phase shifts of the negative pion scattering^{3,4} that the Coulomb interference effect is minor. The forward-scattering correction was therefore made by extrapolating the measured elastic scattering cross section^{3,4} to zero degrees, without Coulomb forces, and taking for the average forward solid angle that subtended by the last counter at the center of the hydrogen. The size of the correction, taking account of the forward-scattered recoil protons as well as mesons, is indicated in column 6 of Table IV and amounts roughly to 3 mb out of a total cross section ranging from 40 to 65 mb.

For the sake of comparison, most of the experiments with the positive pions were made with essentially the same geometry as just described for the negative pions. The geometry, labeled P.H. (for pulse height), differs from the π^- in having a more favorable angle δ , 7.5° instead of 4° . This was made possible by the introduction of the large 20-cm diameter plastic scintillation counter described earlier. Unfortunately, the correction for the forward scattering of π^+ is much less certain than the corresponding correction for the π^- since the available data¹⁸ on the angular distribution of the positive pion scattering are not as precise. In addition, the correction is relatively more serious since the elastic scattering of the π^+ accounts for all the interaction, while for the π^- the elastic scattering contributes roughly only one third of the total cross section, the

charge exchange scattering being more important.^{3,4} The extent of the uncertainty is indicated in Table VII, where the forward scattering correction is listed for two widely different assumed angular distributions: (1) isotropic in the center-of-mass system, and (2) $1+3\cos^2\theta$. In the geometry characterized by the 13° half-angle, the difference in the forwarding scattering correction according to the distribution (1) and (2) is more than the estimated uncertainty in the cross section due to all other causes.

For this reason it was decided to make some experiments in the last geometry listed in Table II with half-angle 6.4° , less conservative in regard to the Coulomb interference effect, but safer insofar as the forward scattering correction itself is smaller. Estimates using the π^+ scattering phase shifts of Homa *et al.*¹⁸ and Glicksman⁴ show that even at 6.4° the Coulomb interference effect is not very serious. At 170 Mev, for example, the true cross section for nuclear scattering through an angle greater than 6.4° probably differs from the corresponding cross section including the Coulomb effect by not more than 2 or 3 millibarns. The total forward scattering correction for the 6.4° geometry is shown in Table VII at 171 Mev and 196 Mev. The difference between the isotropic and $1+3\cos^2\theta$ distributions is of course greatly reduced. By comparing with the results at 171 Mev using the 13° geometry it is evident that the correction based on $1+3\cos^2\theta$ is nearer to the truth.

III. TOTAL CROSS SECTIONS OF NEGATIVE PIONS IN HYDROGEN

In Table III we have listed the primary transmission data from which the total cross sections are eventually

TABLE III. Transmission data for negative pions in hydrogen.

Energy Mev	Absorber	Triples counts	Quadruples counts	Q/T	σ (uncor- rected) 10^{-27} cm ²
133 \pm 7	Dummy Hydrogen	351 067	334 629	0.95317 \pm 0.00037	38.7 \pm 1.1
		350 405	327 447	0.93448 \pm 0.00043	
152 \pm 13	C CH ₂	551 103	466 805	0.84703 \pm 0.00053	52.0 \pm 1.6
		450 782	371 429	0.82396 \pm 0.00063	
157 \pm 8	Dummy Hydrogen	956 691	912 420	0.95372 \pm 0.00022	53.0 \pm 0.8
		1 000 147	928 391	0.92825 \pm 0.00027	
179 \pm 8	Dummy Hydrogen	471 553	450 944	0.95629 \pm 0.00031	58.7 \pm 1.0
		405 844	376 639	0.92803 \pm 0.00042	
194 \pm 7	Dummy Hydrogen	400 308	382 801	0.95626 \pm 0.00033	56.0 \pm 1.0
		500 024	464 653	0.92926 \pm 0.00038	
195 \pm 7	Dummy Hydrogen	500 176	468 153	0.93597 \pm 0.00036	55.2 \pm 1.0
		500 236	455 200	0.90997 \pm 0.00043	
215 \pm 8	Dummy Hydrogen	451 376	435 282	0.96434 \pm 0.00028	49.1 \pm 0.8
		553 174	520 248	0.94047 \pm 0.00032	
236 \pm 7	Dummy Hydrogen	150 098	144 797	0.96468 \pm 0.00049	40.5 \pm 1.5
		160 377	151 547	0.94494 \pm 0.00059	
240 \pm 7	Dummy Hydrogen	200 069	191 798	0.95865 \pm 0.00045	38.4 \pm 1.4
		199 935	187 954	0.94007 \pm 0.00055	
258 \pm 9	Dummy Hydrogen	60 141	57 439	0.95507 \pm 0.0009	33.3 \pm 2.7
		50 133	47 073	0.93896 \pm 0.0011	

¹⁸ Homa, Goldhaber, and Lederman, Phys. Rev. **93**, 554 (1954); R. A. Grandey and A. F. Clark, Phys. Rev. **94**, 766(A) (1954); Orear, Tsao, Lord, and Weaver, Phys. Rev. **95**, 624(A) (1954); Fowler, Lea, Shephard, Shutt, Thorndike, and Whittemore, Phys. Rev. **92**, 832 (1953). [The mean energy of the pions has been revised downward from 260 Mev to about 230 Mev (private communication).]

obtained. For each energy investigated¹⁹ we give the transmission Q/T measured with hydrogen absorber and with an empty styrofoam box (dummy), or, as in the case of the 152-Mev point, with CH_2 and C absorbers. The quoted uncertainty in the transmissions is based entirely on counting statistics.²⁰ The last column of Table III contains the *apparent* or uncorrected cross section given by Eq. (1).

The *experimental* cross section for the geometry used, that is, the proper cross section for removing charged particles from the acceptance cone of the last counter, is obtained only after appropriate corrections are made. Most of these corrections have been mentioned already. Following are the effects to be considered.

(1) Muon contamination. The 5 to 10 percent dilution of the incident beam caused by the presence of muons results in a decrease of the apparent cross section assuming that the muons have no nuclear interaction with hydrogen. For small contaminations we may correct for this by dividing the apparent cross section by the fraction of pions in the beam. The muon contaminations listed in column 3 of Table IV we regard as uncertain to 2 or 3 percent due to inherent difficulties in interpreting the range curve. The electron contamination is considered negligible.

(2) Accidental coincidences. These have been discussed under Background in Sec. I C. On account of background events in the quadruples, the apparent cross section must be increased by the fraction indicated in column 4 of Table IV.

(3) There are a number of other small effects that could be listed. For example, there is a small contribution to the attenuation due to those pion decays, occurring after the monitor, which give rise to muons falling outside the last counter. Since the decay probability depends on the pion energy, this contribution is changed slightly by the additional 4-Mev energy loss when the hydrogen absorber is present. However, with

TABLE IV. Cross sections for negative pions in hydrogen.

Energy Mev	σ (uncor- rected) 10^{-27} cm^2	μ contami- nation percent	Acci- dental percent	σ (exp) 10^{-27} cm^2	Forward scat- tering 10^{-27} cm^2	σ (cor- rected) 10^{-27} cm^2
133 \pm 7	38.7 \pm 1.1	11.0	0.8	43.8 \pm 2.2	3.1	46.9 \pm 2.4
152 \pm 13	52.0 \pm 1.6	8.6	1.0	57.5 \pm 2.8	3.2	60.7 \pm 3.0
157 \pm 8	53.0 \pm 0.8	8.6	3.0	59.7 \pm 2.2	3.2	62.9 \pm 2.4
179 \pm 8	58.7 \pm 1.0	5.5	0.8	62.6 \pm 2.3	3.3	65.9 \pm 2.5
194 \pm 7	56.0 \pm 1.0	5.4	3.4	61.2 \pm 2.3	3.4	64.6 \pm 2.5
195 \pm 7	55.2 \pm 1.0	4.3	3.5	59.7 \pm 2.3	3.4	63.1 \pm 2.5
215 \pm 8	49.1 \pm 0.8	4.5	1.6	52.2 \pm 2.0	3.3	55.5 \pm 2.2
236 \pm 7	40.5 \pm 1.5	4.3	1.5	43.0 \pm 2.2	3.1	46.1 \pm 2.4
240 \pm 7	38.4 \pm 1.4	4.0	1.0	40.4 \pm 2.1	3.1	43.5 \pm 2.3
258 \pm 9	33.3 \pm 2.7	4.6	1.0	35.2 \pm 3.1	3.0	38.2 \pm 3.4

¹⁹ The energy quoted is the mean energy of the pion in the center of the absorber, and the energy spread is compounded from the spread in the incident beam, as estimated from the range curve, and the energy loss in the absorber.

²⁰ If T is the given number of triples, Q the number of quadruples, and p the probability that a meson is transmitted, the root-mean-square fluctuation in Q is $\Delta Q = [T(1-p)p]^{\frac{1}{2}}$. Very nearly, $\Delta Q = [T(1-p)]^{\frac{1}{2}} = [T-Q]^{\frac{1}{2}}$ for p close to unity.

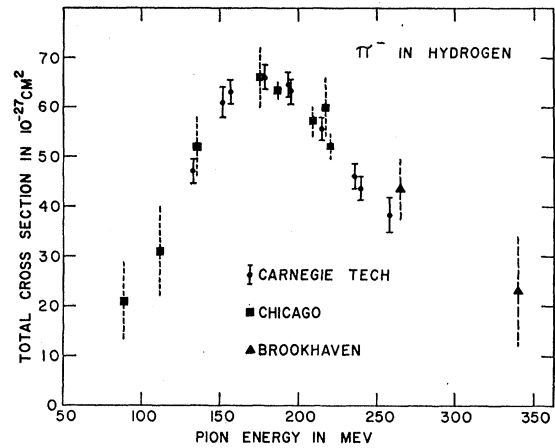


FIG. 5. Total cross sections for negative pions in hydrogen. The Chicago points at 89, 112, 135, 176, and 217 Mev represent the transmission measurements of Anderson *et al.* (reference 2). The Chicago points at 187, 209, and 220 Mev represent transmission measurements of Glicksman (reference 4). The Brookhaven points at 265 Mev and 340 Mev give the results of transmission measurements of Yuan and Lindenbaum (reference 22); these points have energy spreads of ± 30 Mev and ± 40 Mev, respectively.

the geometry used and the measured beam divergence shown in Fig. 2 only a negligible fraction of the muons miss the last counter, and the effect is quite unimportant. Similarly all other effects due to the divergence of the beam are unimportant. We are also justified in neglecting any corrections for γ rays converted in the hydrogen chamber or the last counter, or for neutrons which may give recoil protons in the hydrogen or be counted in the last counter.

The resulting experimental cross section is given in column 5 of Table IV with the error compounded out of the statistical error in the uncorrected cross section and the estimated errors in the corrections. There is left finally the correction for the forward scattering as discussed in detail in Sec. II. The best estimate, based on the available angular distributions,^{3,4} is given in column 6.

The final cross sections, $\sigma_H(\pi^-)$, after all corrections have been made, are listed in the last column of Table IV, with an estimate of the total error.²¹ Figure 5 shows the comparison of the present measurements with those of other laboratories. In general there is good agreement with the original transmission measurements of Anderson, Fermi, *et al.*² and also with the more recent results of Glicksman.⁴ The Brookhaven measurement²² at 265 Mev appears to be somewhat above the curve extrapolated from the present lower energy data. The maximum in the cross section, clearly exhibited by the data, occurs near 180 Mev.

²¹ If we assume that there is unlikely to be a systematic error varying strongly with meson energy, we may get an idea of the relative accuracy of the results from the statistical errors quoted in column 2, Table IV.

²² L. Yuan and S. J. Lindenbaum, Phys. Rev. **93**, 917 (A) (1954) and *Proceedings of Fourth Annual Conference on High Energy Physics* (University of Rochester Press, Rochester, 1954).

IV. TOTAL CROSS SECTIONS FOR POSITIVE PIONS IN HYDROGEN

The essential new feature of the π^+ measurements, apart from the low intensity of the beams relative to the π^- , was the very large contamination of protons which it was necessary to eliminate. Although it was possible to reduce the contamination very much by appropriate shielding²³ near the cyclotron, the protons remained 5 or 10 times more numerous than the pions in the energetic beams of energy 170 Mev and above.

There would be no real difficulty if *all* of these protons were of nearly the same momentum as the pions. They would then have energies from 40 to 50 Mev and could be removed with a suitable absorber. However, even a few protons of higher energy could be very serious inasmuch as some might penetrate the monitor and reach the detector with the hydrogen target empty, but fail to do so with the target full.²⁴ It was therefore necessary to eliminate the protons completely. We used principally two methods to accomplish this: (A) time-of-flight discrimination against protons in the monitor and (B) pulse-height discrimination in the detecting counter.

A. Time-of-Flight Method

With 220-cm distance between first and last monitor counters, as shown in Fig. 6, the time of flight difference between protons and pions of the same momentum is between 20 and 25 μsec , depending on the pion energy and the proton energy loss in the first two counters. There is a difference of about 12 μsec for protons of 65 Mev, which are just stopped by ionization loss in the monitor and the liquid hydrogen. Pulses separated

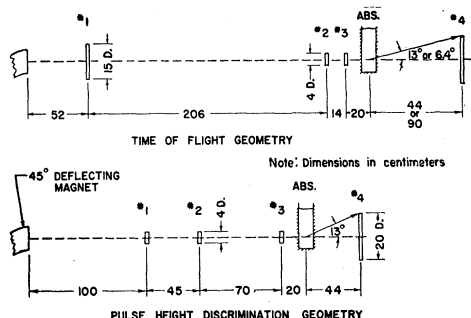


FIG. 6. Geometries for the π^+ measurements.

²³ Since the protons lose more momentum than the pions by ionization loss in the air, those coming from the meson target, with the proper momentum to eventually follow the pions through the external deflecting magnet, must have somewhat different trajectories than the pions near the cyclotron. This makes it possible with shielding to cut out a very large fraction of the protons without materially affecting the pion intensity. Thus, for the 170-Mev beam, the protons were more numerous than the pions by a factor of 100. Insertion of lead shielding reduced this factor to 4.

²⁴ Suppose, for example, that for each 100 pions traversing the monitor, there are 500 protons incident of which, on the average, one has the above-mentioned disagreeable property. Since on the average only 8 of the pions are removed by the hydrogen, we would find too large a cross section by over 10 percent.

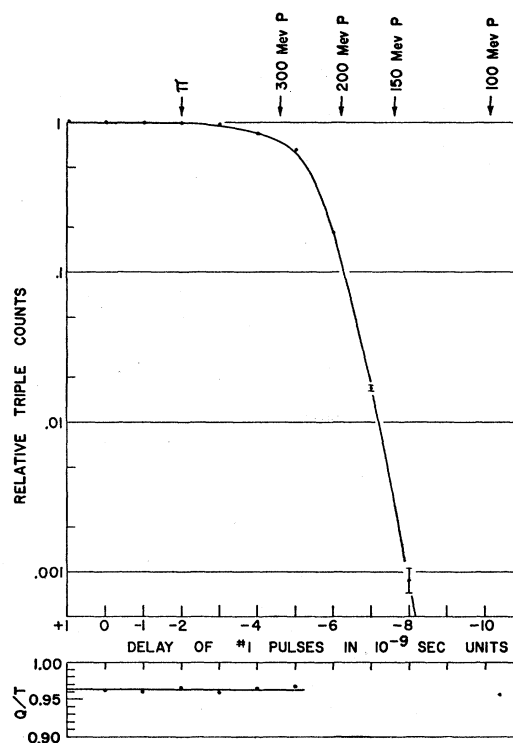


FIG. 7. Response of the monitor coincidence circuit to pulses in delayed coincidence and the transmission Q/T as a function of delay. The arrow labeled π indicates the operating point for pions; the displacements of the arrows labeled P , relative to the π , give the time-of-flight differences between the pions and protons of various energies.

in time by this much are easily rejected by the monitor coincidence circuit. This is clear from Fig. 7, which shows the response of the circuit to monitor pulses in delayed coincidence and also the transmission Q/T for each delay. It is evidently possible to find an operating point for which mesons are counted with 100 percent efficiency while pulses in delayed coincidence by 6 μsec or more (corresponding to protons of 140 Mev or less) are for practical purposes completely rejected.

B. Pulse-Height Method

It may be expected that the penetrating protons,²⁵ because they are slower than the pions, will give appreciably larger pulses in the last counter. We therefore attempted pulse height discrimination using the special 20-cm diameter counter described earlier and the Tektronix 517 oscilloscope as an improvised integral pulse height analyzer.²⁶

Figure 8 shows the pulse-height spectrum for the 171-Mev π^+ experiment, with no hydrogen in the target. The small residue of large pulses should contain

²⁵ The protons with the same momentum as the pions were stopped by ionization loss in an absorber before the monitor.

²⁶ The quadruples coincidence output was used to trigger the sweep and all pulses above a certain height were counted with a photomultiplier viewing the oscilloscope screen.

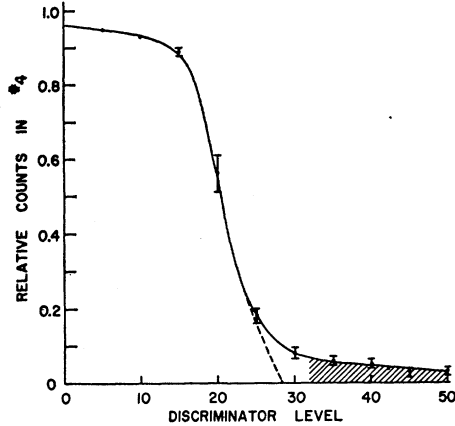


FIG. 8. Integral pulse height spectrum of coincident pulses in the last counter (171-Mev π^+ beam). Pulses in the shaded region were separately counted (called B pulses in Table VI, column 5) and subtracted from the total number of quadruples.

all those due to the penetrating protons and in addition, the relatively more numerous star pulses originated by pions in the counter or the adjacent light pipe. With the hydrogen present there are also large pulses caused by the recoil protons projected in the forward direction. The procedure followed was to reject all quadruple coincidences, with and without hydrogen in which the pulses in the detecting counter were larger than a certain limit set rather arbitrarily by examining the pulse height spectrum. Rejection of the star-producing pions does not alter the cross section since the fraction rejected is the same with and without the hydrogen. Rejection of the recoil protons makes it unnecessary to correct the experimental cross section on that account.

This method is open to the criticism that there is no unique division in the pulse-height spectrum between the meson pulses and the "large" pulses. One could attempt to show that the resulting cross section is essentially independent of the dividing line chosen, but

TABLE V. Transmission data for positive pions in hydrogen by time-of-flight method.

Energy Mev	Absorber	Triples counts	Quad-ruples counts	Q/T	σ (uncorrected) 10^{-27} cm^2
135 \pm 6	Dummy Hydrogen	190 016 100 010	181 609 90 656	0.9557 \pm 0.0005 0.9065 \pm 0.0010	103.5 \pm 2
152 \pm 12	C CH ₂	64 007 80 008	53 940 62 431	0.8427 \pm 0.0017 0.7803 \pm 0.0019	145 \pm 5
156 \pm 6	Dummy Hydrogen	60 004 60 010	57 374 53 379	0.9562 \pm 0.0008 0.8895 \pm 0.0014	142 \pm 3.5
166 \pm 12	C CH ₂	64 010 54 002	54 489 42 433	0.8511 \pm 0.0017 0.7858 \pm 0.0023	150 \pm 5.5
171 \pm 6	Dummy Hydrogen	36 005 40 004	34 515 35 385	0.9586 \pm 0.0011 0.8845 \pm 0.0017	157 \pm 4
171 \pm 6	Dummy Hydrogen $\left. \begin{array}{l} 6.4^\circ \end{array} \right\}$	37 002 40 002	34 431 33 885	0.9305 \pm 0.0014 0.8471 \pm 0.0020	184 \pm 5
185 \pm 8	Dummy Hydrogen	15 506 18 000	14 899 16 016	0.9609 \pm 0.0016 0.8898 \pm 0.0024	151 \pm 6
196 \pm 8	Dummy Hydrogen $\left. \begin{array}{l} 6.4^\circ \end{array} \right\}$	12 830 9 508	12 013 8 107	0.9363 \pm 0.0023 0.8527 \pm 0.0042	183 \pm 9

this becomes too difficult with the very weak π^+ beams at high energy. For this reason we prefer to rely more on the time of flight method, about which there can be little question, using the observed agreement between the results (see below) as an indication that there are no serious systematic errors in either procedure.

C. Results

Table V gives the transmission data and the uncorrected cross sections obtained with the time-of-flight method. Table VII contains the final corrected cross sections including the correction for forward scattering as discussed in Sec. II. The energy range from 135 Mev to 196 Mev has been covered in more or less uniform steps using mostly liquid hydrogen as absorber, with checks using the polyethylene-carbon difference at 152 Mev and 166 Mev.

Table VI contains the transmission data obtained by the pulse-height method, with column 4 giving all the

TABLE VI. Transmission data for positive pions in hydrogen by pulse-height method.

Energy Mev	Absorber	Triples counts T	Quad-ruples counts Q	B counts*	$\frac{Q-B}{T}$	σ (uncorrected) 10^{-27} cm^2
128 \pm 6	Dummy Hydrogen	40 070 35 600	37 975 32 083	...	0.9477 \pm 0.0012 0.9012 \pm 0.0017	98.5 \pm 4
142 \pm 6	Dummy Hydrogen	45 558 45 340	43 013 40 211	...	0.9441 \pm 0.0011 0.8869 \pm 0.0016	122 \pm 4
	C CH ₂	61 005 61 000	51 419 47 301	4492 4475	0.7692 \pm 0.0020 0.7020 \pm 0.0024	172 \pm 6
166 \pm 13	C' (none)	56 006 6 001	44 626 5 813	...	0.7968 \pm 0.0024 0.9686 \pm 0.0023	151 \pm 9
171 \pm 8	Dummy Hydrogen	45 002 46 007	42 726 40 080	2842 3021	0.8862 \pm 0.0016 0.8055 \pm 0.0020	187 \pm 5
182 \pm 9	Dummy Hydrogen	8 277 11 836	7 681 10 072	646 746	0.8499 \pm 0.0042 0.7879 \pm 0.0042	148 \pm 12

* B is the associated number of large detector pulses.

quadruple counts Q and column 5 the associated number of large detector pulses B . At 128 Mev and 142 Mev we have included points taken with no precaution against the penetrating protons; it is apparent from Table VII that the cross sections are consistent with the time-of-flight results at neighboring energies. At 166 Mev we have also included a point taken with polyethylene and carbon absorbers of the same stopping power, since in this case the cross section should in first approximation be independent of the penetrating proton contamination.

All of the results, with an indication of the method and the geometry (either 13° or 6.4° half-angle), are assembled in Table VII and plotted in Fig. 9. The graph shows only the values corrected according to the $1+3 \cos^2\theta$ distribution in the center-of-mass system, since the comparison of the two geometries at 171 Mev seems to indicate that this is more realistic. There is evidently no systematic difference between the results obtained with the two methods.

Figure 10 shows the relation of the present measurements to those of other laboratories. There is satisfactory agreement with the original transmission measurements of Anderson *et al.*²⁷ at Chicago and with photographic plate measurements of Grandey and Clark¹⁸ at Carnegie Tech and Orear *et al.*¹⁸ at Chicago. The photographic measurements of Homa *et al.*¹⁸ at Columbia and the transmission measurements of Yuan and Lindenbaum²² at Brookhaven give values somewhat lower than ours.

V. DISCUSSION OF THE HYDROGEN CROSS SECTIONS

Under the assumption that the total isobaric spin of the pion-nucleon system is conserved by the pion-nucleon interaction, it is possible to analyze the present data for the relative importance of the different isobaric spin states which are involved. If $\sigma(\frac{3}{2})$ and $\sigma(\frac{1}{2})$ denote, respectively, the total cross sections for pion-nucleon interaction in the isobaric spin states $\frac{3}{2}$ and $\frac{1}{2}$, it is

TABLE VII. Cross sections for positive pions in hydrogen.

Energy MeV	σ (un- corr.) 10^{-27} cm ²	μ con- tam. per- cent	Ac- cid. per- cent	σ (exp) 10^{-27} cm ²	σ (corrected) 10^{-27} cm ² (iso- tropic) (1+3 cos ² θ)	Method ^a
128±6	98.5	8	0.7	108±5	115±7	122±8 (as for π ⁻)
135±6	103.5	7	0.5	112±4	119±4	126±4 T. of F.
142±6	122	7	0.7	132±5	143±7	150±8 (as for π ⁻)
152±12	145	5	0.3	153±6	165±6	175±6 T. of F.
156±6	142	5	0.5	150±5	160±5	170±5 T. of F.
166±13	172	7.5	0.6	187±9	191±10	194±12 P.H.
166±12	150	7.5	0.6	164±11	176±11	188±11 thick carbon
171±8	157	7.5	0.3	163±7	175±7	187±7 T. of F.
171±6	187	7.5	0.3	203±8	207±10	210±12 P.H.
171±6	157	7	0.5	170±6	184±6	196±6 T. of F.
182±9	184	7	0.5	199±6	202±6	205±6 T. of F. (6.4°)
182±9	143	7	0.3	160±14	164±18	166±20 P.H.
185±8	151	6	0.5	161±8	176±8	188±8 T. of F.
196±8	183	7	0	197±14	200±14	202±14 T. of F. (6.4°)

^a T. of F. = time-of-flight method; P.H. = pulse-height method.

easily verified that²⁸

$$\sigma(\frac{3}{2}) = \sigma(\pi^+ + p), \quad (2)$$

$$\sigma(\frac{1}{2}) = \frac{1}{2}[3\sigma(\pi^- + p) - \sigma(\pi^+ + p)]. \quad (3)$$

Figure 9 and Fig. 10 show a comparison of $3\sigma(\pi^- + p)$ with $\sigma(\pi^+ + p)$ based on the data of this experiment. The permissible range of the negative pion cross section is indicated by the two dotted curves. It is apparent that within the experimental accuracy, the positive pion cross sections lie between the dotted curves, with deviations that show no systematic trend. The measurements therefore indicate that in the energy range from 130 Mev to 200 Mev the cross section $\sigma(\frac{1}{2})$ is very small.

²⁷ Anderson, Fermi, Long, and Nagle, Phys. Rev. **85**, 936 (1952).

²⁸ In these relations the $\pi^- + p$ total cross section should not include the cross section for radiative capture: $\pi^- + p \rightarrow n + \gamma$. For the energy range of the present measurements, the radiative cross section is 0.5 mb or less, as estimated from the photopion production data of J. Steinberger and A. S. Bishop, Phys. Rev. **86**, 171 (1952), and White, Jacobson, and Schulz, Phys. Rev. **88**, 836 (1952). In view of the other errors, this correction has not been made.

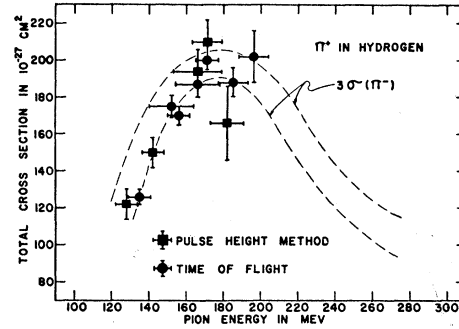


FIG. 9. Total cross sections for π^+ mesons in hydrogen; comparison of time-of-flight and pulse-height methods. The dotted curves show the permissible range of variation of three times the total cross section for π^- mesons, based on the data of this experiment (Fig. 5).

Assuming that $\sigma(\frac{1}{2})$ is small also up to 260 Mev, we may take the energy variation of the negative pion total cross section as indicating the behavior of the cross section $\sigma(\frac{3}{2})$ (multiplied by one third). It has been suggested on theoretical grounds²⁹ that the maximum in the cross section is due to an especially strong interaction in the pion-nucleon P -state of total angular momentum $\frac{3}{2}$. To see if this hypothesis is consistent with the data, we may compare the negative pion total cross section with the maximum possible contribution of the state $I = \frac{3}{2}, J = \frac{3}{2}, L = 1$. For a phase shift of 90° in this state, the partial cross section which it contributes is $(8/3)\pi\lambda^2$, where λ is the de Broglie wavelength of the pion in the c.m. system. The dotted curve in Fig. 11 shows $(8/3)\pi\lambda^2$ over the energy range of the

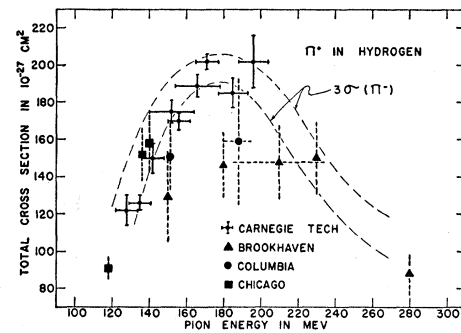


FIG. 10. Comparison of total cross sections for π^+ mesons in hydrogen with results from other laboratories. The Chicago points at 118 Mev and 136 Mev represent the transmission measurements of Anderson *et al.* (reference 27). The Chicago point at 140 Mev represents the photographic measurement of Orear *et al.* (reference 18). The point at 151 Mev gives the combination of photographic measurements of Grandey and Clark at Carnegie Tech with Homa *et al.* (reference 18) of Columbia. The Columbia point at 188 Mev is also due to Homa *et al.* (reference 18). The Brookhaven points at 150 Mev, 180 Mev, 210 Mev, and 280 Mev give the preliminary results of transmission measurements of Yuan and Lindenbaum (reference 22); the point at the revised energy of 230 Mev (with a rather large energy spread) is a result of the cloud chamber measurements of Fowler *et al.* (reference 18). Typical energy spreads are shown on one point each for Columbia and Brookhaven measurements.

²⁹ K. A. Brueckner, Phys. Rev. **86**, 106 (1952).

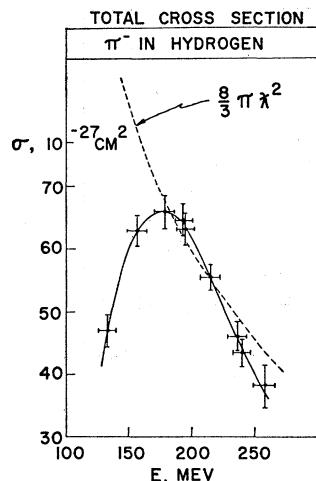


FIG. 11. Comparison of the cross section for π^- mesons in hydrogen with $(8/3)\pi\lambda^2$.

measurements. In the energy interval 185 Mev to 215 Mev, the curve drawn through the experimental points lies above the curve of $(8/3)\pi\lambda^2$. It is therefore possible that somewhere near 200 Mev the phase shift for the $P_1, I=\frac{3}{2}$ state passes through 90° , with the other states contributing little to the total cross section. From the total cross section measurements alone it is not possible to decide this question.³⁰

VI. DEUTERIUM CROSS SECTIONS

The total cross sections for pions interacting with deuterium are of interest for two reasons. (1) According to the principle of charge symmetry, positive and negative pions should have equal total cross sections. (2) By comparison of the total cross section with the sum of the free-particle cross sections, we may learn something about the interference between the amplitudes scattered by the neutron and the proton in the deuteron.

It would of course be best for such measurements to use a liquid deuterium target. Since this was not available, we measured instead the difference between the deuterium and hydrogen cross sections, comparing the transmission of a D_2O liquid cell with that of an H_2O cell containing the same number of molecules per cm^2 (see Table I). The geometry was kept the same as for most of the measurements with liquid hydrogen; the last counter subtended a cone of half-angle 13° at the center of the absorber.

The experimental difference cross sections σ_{D-H} , corrected for everything except the forward scattering of charged particles into the 13° cone, are given in the

³⁰ Extensive analysis by de Hoffmann, Metropolis, Alei, and Bethe, by R. L. Martin (private communication), and by Glicksman⁴ of the angular distribution of the negative pion scattering as a function of energy, taken in conjunction with the present measurements of positive pion total cross sections, has shown that there exists a consistent set of scattering phase shifts which includes a passage through 90° for the $P_1, I=\frac{3}{2}$ phase shift, near 195 Mev. Nevertheless, this solution is not unique, mainly because of the scarcity of experimental information on the differential positive-pion cross section in this energy range.

second columns of Table VIII and Table IX for positive and negative pions, respectively. In the measurements with the positive pions, the accompanying protons having the same momentum as the pions were in most cases eliminated by placing a suitable thickness of Lucite before the monitor. Since the H_2O and D_2O cells have the same stopping power, the possible small remnant of more energetic protons is of no importance. At the highest energy, 181 Mev, the time-of-flight method was used. The poor statistical accuracy of the positive pion results is due to the small measured difference in the transmissions of D_2O and H_2O . By adding the experimental cross section in hydrogen, for the 13° geometry, to the experimental difference cross section σ_{D-H} we obtain the experimental total cross section for deuterium as indicated in the fourth columns of Table VIII and Table IX.

Before examining the data from the standpoint of charge symmetry, it is essential to make some guess about the forward scattering. The existing experimental information^{31,32} does not cover the range of small angles of interest to us. We have therefore used a theoretical estimate of Brueckner,³³ based on the impulse approxi-

TABLE VIII. Deuterium cross sections for positive pions.

Energy Mev	σ_{D-H} (exp) $10^{-27} cm^2$	σ_H (exp) $10^{-27} cm^2$	σ_D (exp) $10^{-27} cm^2$	π^+ for- ward 10^{-27} cm^2	p for- ward 10^{-27} cm^2	$\sigma_D(\pi^+)$ $10^{-27} cm^2$
123±12	26±4	96±8	122±9	13	5	140±9
137±12	31±5	120±8	151±9	17	6	174±9
162±12	25±11	162±8	187±14	20	10	217±14
181±13	32±14	170±8	202±16	24	11	237±16

mation and taking account of the rescattering of the outgoing meson waves from one nucleon by the other nucleon in the deuteron. According to this estimate there is a rather pronounced forward peak of pions which are scattered elastically by the deuteron. It seems reasonable to assume a forward peak of comparable magnitude for the inelastically scattered pions as well. The fifth columns of Table VIII and Table IX give the cross sections for nuclear scattering of the pions into the 13° forward cone, obtained on this basis. The scattering cross sections of positive and negative pions have been taken equal in accordance with the principle of charge symmetry. Deuterons scattered in the forward direction seem to be relatively unimportant^{31,33} and have been neglected.

For protons scattered forward, we can expect a difference between the positive and negative pion experiments, since the neutron and proton are expected to exchange roles in the interaction. A possible estimate

³¹ Arase, Goldhaber, and Goldhaber, Phys. Rev. **90**, 160 (1953).

³² D. E. Nagle, Phys. Rev. **93**, 918 (A) (1954).

³³ K. A. Brueckner, Phys. Rev. **89**, 834 (1953); **90**, 715 (1953). We wish to thank Dr. Brueckner for discussion of the deuterium scattering.

might be based on the free pion-proton (or pion-neutron) differential cross sections for the case that the pion is scattered backward (or, for positive pions incident, that a neutral pion emerges backward). However, the theoretical indication³³ is that the cross section is reduced from the free particle approximation by the multiple scattering of the pion between the nucleons in the deuteron, as well as other effects neglected in the impulse approximation. We might also expect the angular distribution of backward, inelastically scattered pions to be less peaked than it may be for the scattering by a free nucleon. For these reasons we have corrected for protons scattered forward by taking, rather arbitrarily, one-half of the estimate based on the free pion-proton, or pion-neutron differential cross sections. The corresponding cross sections are listed in the sixth columns of Table VIII and Table IX.

The last columns of Table VIII and Table IX contain our estimates of the total cross section for positive or negative pions interacting with deuterium. The errors indicated are due only to statistics and uncertainties

TABLE IX. Deuterium cross sections for negative pions.

Energy Mev	σ_{D-H} (exp) 10^{-27} cm ²	σ_H (exp) 10^{-27} cm ²	σ_D (exp) 10^{-27} cm ²	π^- for- ward 10^{-27} cm ²	ϕ for- ward 10^{-27} cm ²	$\sigma_D(\pi^-)$ 10^{-27} cm ²
128±12	95±5	40±3	135±6	14	0.5	150±6
152±13	117±5	58±3	175±6	19	1	195±6
175±13	133±4	63±3	196±5	23	1	220±5
189±12	132±4	62±3	194±5	26	1	221±5
210±13	125±5	55±3	180±6	25	1	206±6
231±12	107±4	46±3	153±5	23	1	177±5

in the μ contamination and background. The uncertainties in the corrections for forward scattering are no doubt larger but difficult to assign.

As may be seen in Fig. 12, the results are consistent with the requirement of charge symmetry, but, in view of the large uncertainties in the corrections, cannot provide a completely convincing demonstration. From the comparison with the sum of the free-particle cross sections also shown in Fig. 12, it is clear that the deuteron scatters less than would be indicated on the assumption of incoherent scattering from the neutron and proton. This difference becomes somewhat more pronounced if the absorption cross section for the reaction, pion+deuteron→nucleon+nucleon,³⁴ is subtracted from the measured total cross section to give a total scattering cross section of the deuteron 10 or 15

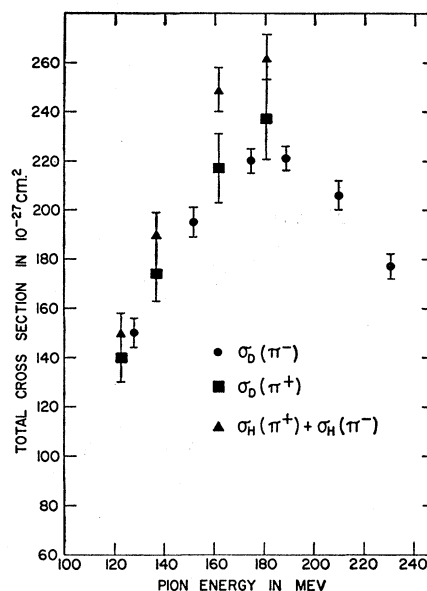


FIG. 12. Deuterium total cross sections for positive and negative pions.

mb lower, depending on how one extrapolates the lower energy data.³⁴ Brueckner³³ has shown, by using a model for the multiple scattering of the meson within the deuteron, that such a depression of the deuteron scattering cross section may be expected even though the waves scattered singly by the neutron or proton may interfere constructively.

The earlier measurements of the deuterium cross sections, made at Chicago,³⁵ and the results reported here are consistent with each other, although the corrections for the forward scattering have been made somewhat differently.

ACKNOWLEDGMENT

It is a pleasure to thank Dr. Simeon Friedberg and Dr. James Zimmerman of the Carnegie Tech Low-Temperature Laboratory for expert advice on the production and handling of liquid hydrogen. We are especially grateful to Mr. James Thompson and Mr. Homer Collins for their efforts to keep the cyclotron in good running order and for excellent technical advice on many problems. The active cooperation of Dr. Lloyd Smith in the initial experiments with the meson beams was an important factor in getting these experiments under way.

³⁴ Durbin, Loar, and Steinberger, Phys. Rev. **84**, 581 (1951).

³⁵ Anderson, Fermi, Nagle, and Yodh, Phys. Rev. **86**, 413 (1952).